

Selective Ligand Modification on the Periphery of Diruthenium Compounds: Toward New Metal-Alkynyl Scaffolds

Wei-Zhong Chen and Tong Ren*

Department of Chemistry, University of Miami, Coral Gables, Florida 33146

Received January 31, 2005

Diruthenium compounds $\text{Ru}_2(\text{DmAniF})_3(\text{OAc})\text{Cl}$ (**1**, *DmAniF* is *N,N'*-di(*m*-methoxyphenyl)-formamidinate) and *cis*- $\text{Ru}_2(\text{DmAniF})_2(\text{OAc})_2\text{Cl}$ (**6**) reacted with *N,N'*-dimethyl-4-iodobenzamidine (HDMBA-I) to furnish new compounds $\text{Ru}_2(\text{DmAniF})_3(\text{DMBA-I})\text{Cl}$ (**2**) and *cis*- $\text{Ru}_2(\text{DmAniF})_2(\text{DMBA-I})_2\text{Cl}$ (**7**), respectively. Both compounds **2** and **7** were modified with a terminal alkyne under Sonogashira conditions. Examples reported include **2** cross-coupled with $\text{HC}\equiv\text{CSi}^i\text{Pr}_3$ or $\text{HC}\equiv\text{CFc}$ to yield $\text{Ru}_2(\text{DmAniF})_3(\text{DMBA-4-C}_2\text{Si}^i\text{Pr}_3)\text{Cl}$ (**3a**) or $\text{Ru}_2(\text{DmAniF})_3(\text{DMBA-4-C}_2\text{Fc})\text{Cl}$ (**3b**), respectively, and **7** cross-coupled with $\text{HC}\equiv\text{CFc}$ to yield *cis*- $\text{Ru}_2(\text{DmAniF})_2(\text{DMBA-4-C}_2\text{Fc})_2\text{Cl}$ (**8**). The peripherally modified compounds (**2**, **3a/3b**, **7**, and **8**) were further alkynylated at the axial positions of the Ru_2 core to yield a series of bis-alkynyl adducts: $\text{Ru}_2(\text{DmAniF})_3(\text{DMBA-4-C}_2\text{Si}^i\text{Pr}_3)(\text{C}_4\text{SiMe}_3)_2$ (**4a**), $\text{Ru}_2(\text{DmAniF})_3(\text{DMBA-4-C}_2\text{Fc})(\text{C}_4\text{SiMe}_3)_2$ (**4b**), $\text{Ru}_2(\text{DmAniF})_3(\text{DMBA-I})(\text{C}_4\text{SiMe}_3)_2$ (**5**), *cis*- $\text{Ru}_2(\text{DmAniF})_2(\text{DMBA-4-C}_2\text{Fc})_2(\text{C}_2\text{Ph})_2$ (**9**), and *cis*- $\text{Ru}_2(\text{DmAniF})_2(\text{DMBA-I})_2(\text{C}_2\text{Ph})_2$ (**10**). All compounds reported were characterized with voltammetric, vis-NIR, and NMR (whenever applicable) techniques. Molecular structures of compounds **1**, **4a**, **5**, **6**, **9**, and **10** were established through X-ray diffraction studies.

Introduction

Transition metal compounds containing σ -alkynyl ligands¹ are fundamentally interesting due to their relevance to both the understanding of metal-carbon covalent bonds^{2,3} and metal-assisted transformation/interconversion among alkynes, vinylidenes, and allenylidenes.⁴ Recent decades have witnessed significant progress in utilizing tailored metal-alkynyl compounds as active species for nonlinear optics,⁵ organic light-emitting diodes (OLED),⁶ molecular sensors,⁷ and molecular wires.⁸ In the latter area, many excellent accounts have appeared based on primarily the linear

$[\text{M}]-(\text{C}\equiv\text{C})_n-[\text{M}]$ type compounds with $[\text{M}]$ as CpRuP_2 and $\text{CpRu}(\text{P}-\text{P})$, where P and P-P stand respectively for mono- and bisphosphines,⁹ $\text{CpReP}(\text{NO})$,¹⁰ $\text{CpFe}(\text{P}-\text{P})$,¹¹ $\text{Mn}(\text{P}-\text{P})_2\text{I}$ and $\text{CpMn}(\text{P}-\text{P})$,¹² and $(\text{C}_6\text{F}_5)\text{PtP}_2$.¹³ While such 1-D systems have been studied extensively, efforts toward 2-D and 3-D metal-alkynyl networks remain very limited. Notable examples include the tetra- and octanuclear platinum butadiyne squares¹⁴

* To whom correspondence should be addressed. E-mail: tren@miami.edu. Tel: (305) 284-6617. Fax: (305) 284-1880.

(1) *Modern Acetylene Chemistry*; Stang, P. J.; Diederich, F., Eds.; VCH: Weinheim, 1995.

(2) Nast, R. *Coord. Chem. Rev.* **1982**, *47*, 89.

(3) Manna, J.; John, K. D.; Hopkins, M. D. *Adv. Organomet. Chem.* **1995**, *38*, 79.

(4) (a) Bruce, M. I. *Chem. Rev.* **1991**, *91*, 197. (b) Bruce, M. I. *Chem. Rev.* **1998**, *98*, 2797. (c) King, R. B. *Coord. Chem. Rev.* **2004**, *248*, 1531. (d) Bruce, M. I. *Coord. Chem. Rev.* **2004**, *248*, 1603. (e) Rigaut, S.; Touchard, D.; Dixneuf, P. H. *Coord. Chem. Rev.* **2004**, *248*, 1585.

(5) (a) Whittall, I. R.; McDonagh, A. M.; Humphrey, M. G.; Samoc, M. *Adv. Organomet. Chem.* **1998**, *42*, 291. (b) *Adv. Organomet. Chem.* **1999**, *43*, 349. (c) Cifuentes, M. P.; Humphrey, M. G. *J. Organomet. Chem.* **2004**, *689*, 3968. (d) Coe, B. J.; Curati, N. R. *Comm. Inorg. Chem.* **2004**, *25*, 147.

(6) (a) Yam, V. W. *Acc. Chem. Res.* **2002**, *35*, 555. (b) Wadas, T. J.; Lachicotte, R. J.; Eisenberg, R. *Inorg. Chem.* **2003**, *42*, 3772. (c) Tonzetich, Z. J.; Eisenberg, R. *Inorg. Chim. Acta* **2003**, *345*, 340. (d) Lu, W.; Mi, B.-X.; Chan, M. C. W.; Hui, Z.; Zhu, N.; Lee, S.-T.; Che, C.-M. *Chem. Commun.* **2002**, 206.

(7) (a) Yam, V. W. *J. Organomet. Chem.* **2004**, *689*, 1393. (b) Siu, P. K. M.; Lai, S.-W.; Lu, W.; Zhu, N.; Che, C.-M. *Eur. J. Inorg. Chem.* **2003**, 2749. (c) Lu, W.; Chan, M. C. W.; Zhu, N. Y.; Che, C. M.; He, Z.; Wong, K. Y. *Chem. Eur. J.* **2003**, *9*, 6155. (d) Yang, Q.-Z.; Wu, L.-Z.; Zhang, H.; Chen, B.; Wu, Z.-X.; Zhang, L.-P.; Tung, C.-H. *Inorg. Chem.* **2004**, *43*, 5195.

(8) (a) Chisholm, M. H. *Angew. Chem., Int. Ed. Engl.* **1991**, *30*, 673. (b) Bunz, U. H. F. *Angew. Chem., Int. Ed. Engl.* **1996**, *35*, 969. (c) Paul, F.; Lapinte, C. *Coord. Chem. Rev.* **1998**, *178–180*, 431. (d) Paul, F.; Lapinte, C. In *Unusual structures and physical properties in organometallic chemistry*; Gielen, M., Willem, R., Wrackmeyer, B., Eds.; Wiley: West Sussex, 2002. (e) Szafert, S.; Gladysz, J. A. *Chem. Rev.* **2003**, *103*, 4175. (f) Bruce, M. I.; Low, P. J. *Adv. Organomet. Chem.* **2004**, *50*, 179.

(9) (a) Bruce, M. I.; Low, P. J.; Costuas, K.; Halet, J.-F.; Best, S. P.; Heath, G. A. *J. Am. Chem. Soc.* **2000**, *122*, 1949. (b) Bruce, M. I.; Ellis, B. G.; Gaudio, M.; Lapinte, C.; Melino, G.; Paul, F.; Skelton, B. W.; Smith, M. E.; Toupet, L.; White, A. H. *Dalton Trans.* **2004**, 1601.

(10) (a) Dembinski, R.; Lis, T.; Szafert, S.; Mayne, C. L.; Bartik, T.; Gladysz, J. A. *J. Organomet. Chem.* **1999**, *578*, 229. (b) Brady, M.; Weng, W.; Zou, Y.; Seyler, J. W.; Amoroso, A. J.; Arif, A. M.; Bohme, M.; Frenking, G.; Gladysz, J. A. *J. Am. Chem. Soc.* **1997**, *119*, 775. (c) Batrik, T.; Bartik, B.; Brady, M.; Dembinski, R.; Gladysz, J. A. *Angew. Chem., Int. Ed.* **1996**, *35*, 414.

(11) (a) Le Narvor, N.; Lapinte, C. *J. Chem. Soc., Chem. Commun.* **1993**, 357. (b) Le Narvor, N.; Toupet, L.; Lapinte, C. *J. Am. Chem. Soc.* **1995**, *117*, 7129. (c) Coat, F.; Lapinte, C. *Organometallics* **1996**, *15*, 477. (d) Coat, F.; Paul, F.; Lapinte, C.; Toupet, L.; Costuas, K.; Halet, J.-F. *J. Organomet. Chem.* **2003**, *683*, 368.

(12) (a) Kheradmandan, S.; Venkatesan, K.; Blacque, O.; Schmalle, H. W.; Berke, H. *Chem. Eur. J.* **2004**, *10*, 4872. (b) Kheradmandan, S.; Heinze, K.; Schmalle, H. W.; Berke, H. *Angew. Chem., Int. Ed.* **1999**, *38*, 2270. (c) Fernández, F. J.; Blacque, O.; Alfonso, M.; Berke, H. *Chem. Commun.* **2001**, 1266.

(13) (a) Mohr, W.; Stahl, J.; Hampel, F.; Gladysz, J. A. *Inorg. Chem.* **2001**, *40*, 3263. (b) Stahl, J.; Bohling, J. C.; Bauer, E. B.; Peters, T. B.; Mohr, W.; Martín-Alvarez, J. M.; Hampel, F.; Gladysz, J. A. *Angew. Chem., Int. Ed.* **2002**, *41*, 1871. (c) Mohr, W.; Stahl, J.; Hampel, F.; Gladysz, J. A. *Chem. Eur. J.* **2003**, *9*, 3324.

and Pt- and Ru-acetylide dendrimers.¹⁵ In contrast, 2-D and 3-D architectures based on both *organic* polyethynylated π -systems and their metal π -complexes have been systematically explored by a number of laboratories.¹⁶ In addition to their rich structural features and interesting physical properties displayed, organic polyethynylated compounds are necessary precursors for fused nonplanar aromatic compounds including fullerenes.¹⁷ Clearly, diversified topological features and unusual physical properties should be expected from the systematic incorporation of transition metal units into 2-D and 3-D carbon-rich networks.

Diruthenium paddlewheel compounds bearing one or two alkynyl ligands at the axial positions, first discovered by Cotton et al. in 1986,¹⁸ have been carefully examined in recent years by the laboratories of Kadish and Bear¹⁹ and Ren.²⁰ Ru₂-alkynyl compounds would be of interest as building blocks for supramolecular materials as well, since they are both intense visible–near-infrared (vis–NIR) chromophores and excellent electrophores with multiple reversible redox couples over a broad potential window.²¹ Noteworthy recent results from our laboratory include the demonstration of high *electron* mobility across both polyyn-diyls²² and (*E*)-hex-3-ene-1,5-diyn-diyl²³ bridges between two Ru₂ termini and facile *hole* transfer between two ferrocenyl groups across a Ru₂ unit along the axial direction.²⁴ To retain the chromophoric and electrophoric features

when incorporated into 2-D and 3-D supramolecular assemblies, Ru₂-alkynyl compounds need to be functionalized in the direction(s) orthogonal to the Ru₂– σ alkynyl vector.

Availability of Ru₂(LL)_{4–n}(OAc)_n type compounds (*n* = 1, 2, or 3, LL is a *N,N'*-bidentate ligand) opens the door to selective functionalization of diruthenium complexes at their periphery. The bridging acetate is labile and can be replaced by better donors such as a *N,N'*-bidentate ligand (LL') that is different from LL to yield Ru₂(LL)_{4–n}(LL')_n type compounds. Recent examples of Ru₂(LL)_{4–n}(OAc)_n type compounds include LL as *N,N'*-di(*o*-methoxyphenyl)formamidinate,²⁵ *N,N'*-diphenylformamidinate (*DPhF*),²⁶ and *N,N'*-di(*p*-anisylformamidinate) (*DpAniF*) as the LL ligand.²⁷ Among these examples, the synthesis of Ru₂(*DPhF*)₃(OAc)Cl by Jiménez-Aparicio et al. is most attractive, where refluxing Ru₂(OAc)₄Cl and 3 equiv of *HDPPhF* in the presence of LiCl and triethylamine afforded Ru₂(*DPhF*)₃(OAc)Cl in 84% yield after simple recrystallization.²⁶ Very recently, synthetic procedures for a complete series of Ru₂-(formamidinate)_{4–n}(OAc)_nCl compounds with *n* = 0–3 were reported in detail, and their utility as building blocks for polymeric architectures was postulated.²⁷ Previously, we communicated that Ru₂(*DmAniF*)₃(OAc)Cl (**1**) reacted readily with *N,N'*-dimethyl-4-iodobenzamide (HDMBA-I) to yield Ru₂(*DmAniF*)₃(DMBA-I)Cl, and the latter enables the peripheral modification via the Sonogoshira coupling reaction.²⁸ In this contribution, we describe both the chemistry of **1** and its surrogates in detail and analogous chemistry based on a new synthon, *cis*-Ru₂(*DmAniF*)₂(OAc)₂Cl.

Result and Discussions

Syntheses. Two important starting compounds, Ru₂-(*DmAniF*)₃(OAc)Cl (**1**) and *cis*-Ru₂(*DmAniF*)₂(OAc)₂Cl (**6**), were prepared using procedures modified from literature.^{26,27} Recently, Angaridis et al. reported that refluxing Ru₂(OAc)₄Cl with 2 equiv of *HDpAniF* in the presence of LiCl and Et₃N for 18 h resulted in *cis*-Ru₂-(*DpAniF*)₂(OAc)₂Cl in 85% yield.²⁷ However, our attempt to prepare **6** under identical conditions resulted in **1** as the major product instead. It was found that a lower reaction temperature (≤ 60 °C) favors the formation of compound **6** as the major product.

As shown in Schemes 1 and 2, acetate ligands in both compounds **1** and **6** can be readily substituted with DMBA-I to furnish Ru₂(*DmAniF*)₃(DMBA-I)Cl (**2**) and *cis*-Ru₂(*DmAniF*)₂(DMBA-I)₂Cl (**7**), respectively, in satisfactory yields. The iodo substituents in the resultant compounds enable peripheral modification through a number of Pd-catalyzed coupling reactions.^{29,30} Hence,

(14) (a) Al-Qaisi, S. M.; Galat, K. J.; Chai, M.; Ray, D. G.; Rinaldi, P. L.; Tessier, C. A.; Youngs, W. J. *J. Am. Chem. Soc.* **1998**, *120*, 12149.

(b) Bruce, M. I.; Costuas, K.; Halet, J.-F.; Hall, B. C.; Low, P. J.; Nicholson, B. K.; Skelton, B. W.; White, A. H. *J. Chem. Soc., Dalton Trans.* **2002**, 383. (c) Janka, M.; Anderson, G. K.; Rath, N. P. *Organometallics* **2004**, *23*, 4382.

(15) (a) Albinati, A.; Leoni, P.; Marchetti, L.; Rizzato, S. *Angew. Chem., Int. Ed.* **2003**, *42*, 5990. (b) Leininger, S.; Stang, P. J.; Huang, S. P. *Organometallics* **1998**, *17*, 3981. (c) Onitsuka, K.; Fujimoto, M.; Oshiro, N.; Takahashi, S. *Angew. Chem., Int. Ed.* **1999**, *38*, 689. (d) Onitsuka, K.; Shimizu, A.; Takahashi, S. *Chem. Commun.* **2003**, 280. (e) Uno, M.; Dixneuf, P. H. *Angew. Chem., Int. Ed.* **1998**, *37*, 1714. (f) Hurst, S. K.; Cifuentes, M. P.; Humphrey, M. G. *Organometallics* **2002**, *21*, 2353. (g) McDonagh, A. M.; Humphrey, M. G.; Samoc, M.; Luther-Davies, B. *Organometallics* **1999**, *18*, 5195.

(16) (a) Bunz, U. H. F. In *Carbon Rich Compounds II*; De Meijere, A., Ed.; Springer-Verlag: Berlin, 1999; Vol. 201, p 131. (b) Diederich, F.; Gobbi, L. In *Carbon Rich Compounds II*; De Meijere, A., Ed.; Springer-Verlag: Berlin, 1999; Vol. 201, p 43. (c) Bunz, U. H. F.; Rubin, Y.; Tobe, Y. *Chem. Soc. Rev.* **1999**, *28*, 107. (d) Bunz, U. H. F. *J. Organomet. Chem.* **2003**, *683*, 269. (e) Diederich, F. *Nature* **1994**, *369*, 199. And the earlier references therein.

(17) (a) Scott, L. T. *Angew. Chem., Int. Ed.* **2004**, *43*, 4994. (b) Hopf, H. *Classics in Hydrocarbon Chemistry*; Wiley-VCH: Weinheim, 2000.

(18) Chakravarty, A. R.; Cotton, F. A. *Inorg. Chim. Acta* **1986**, *113*, 19.

(19) (a) Bear, J. L.; Han, B.; Huang, S.; Kadish, K. M. *Inorg. Chem.* **1996**, *35*, 3012. (b) Bear, J. L.; Han, B.; Huang, S. *J. Am. Chem. Soc.* **1993**, *115*, 1175. (c) Bear, J. L.; Li, Y.; Han, B.; Caemelbecke, E. V.; Kadish, K. M. *Inorg. Chem.* **1997**, *36*, 5449. (d) Kadish, K. M.; Phan, T. D.; Wang, L.-L.; Giribabu, L.; Thuriere, A.; Wellhoff, J.; Huang, S.; Caemelbecke, E. V.; Bear, J. L. *Inorg. Chem.* **2004**, *43*, 4825.

(20) (a) Lin, C.; Ren, T.; Valente, E. J.; Zubkowski, J. D. *J. Chem. Soc., Dalton Trans.* **1998**, 571. (b) Lin, C.; Ren, T.; Valente, E. J.; Zubkowski, J. D. *J. Organomet. Chem.* **1999**, *579*, 114. (c) Zou, G.; Alvarez, J. C.; Ren, T. *J. Organomet. Chem.* **2000**, *596*, 152. (d) Xu, G.-L.; Ren, T. *Inorg. Chem.* **2001**, *40*, 2925. (e) Xu, G.-L.; Ren, T. *Organometallics* **2001**, *20*, 2400. (f) Ren, T. *Organometallics* **2002**, *21*, 732. (g) Xu, G.-L.; Campana, C.; Ren, T. *Inorg. Chem.* **2002**, *41*, 3521. (h) Xu, G.-L.; Ren, T. *J. Organomet. Chem.* **2002**, *655*, 239. (i) Xu, G.-L.; Jablonski, C. G.; Ren, T. *J. Organomet. Chem.* **2003**, *683*, 388. (j) Hurst, S. K.; Xu, G.-L.; Ren, T. *Organometallics* **2003**, *22*, 4118.

(21) Ren, T.; Xu, G.-L. *Comm. Inorg. Chem.* **2002**, *23*, 355. (b) Hurst, S. K.; Ren, T. *J. Organomet. Chem.* **2003**, *670*, 188.

(22) (a) Ren, T.; Zou, G.; Alvarez, J. C. *Chem. Commun.* **2000**, 1197. (b) Xu, G.-L.; Zou, G.; Ni, Y.-H.; DeRosa, M. C.; Crutchley, R. J.; Ren, T. *J. Am. Chem. Soc.* **2003**, *125*, 10057.

(23) Shi, Y.; Yee, G. T.; Wang, G.; Ren, T. *J. Am. Chem. Soc.* **2004**, *126*, 10552.

(24) (a) Xu, G.-L.; DeRosa, M. C.; Crutchley, R. J.; Ren, T. *J. Am. Chem. Soc.* **2004**, *126*, 3728. (b) Xu, G.-L.; DeRosa, M. C.; Crutchley, R. J.; Ren, T. *J. Am. Chem. Soc.* **2005**, *127*, manuscript in preparation.

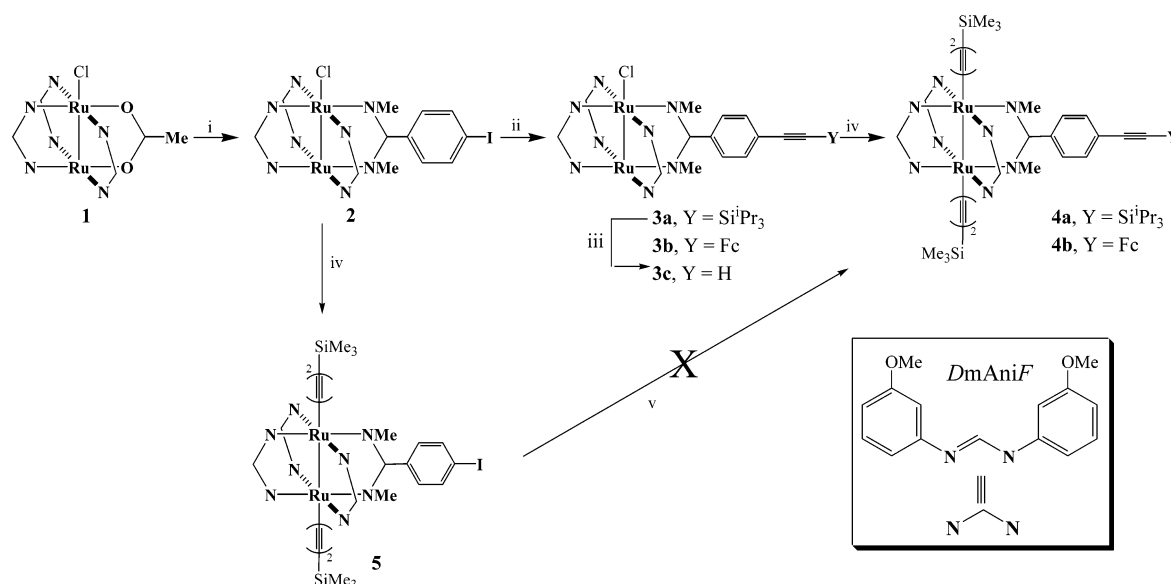
(25) Ren, T.; DeSilva, V.; Zou, G.; Lin, C.; Daniels, L. M.; Campana, C. F.; Alvarez, J. C. *Inorg. Chem. Commun.* **1999**, 2, 301.

(26) Barral, M. C.; Herrero, S.; Jiménez-Aparicio, R.; Torres, M. R.; Urbanos, F. A. *Inorg. Chem. Commun.* **2004**, *7*, 42.

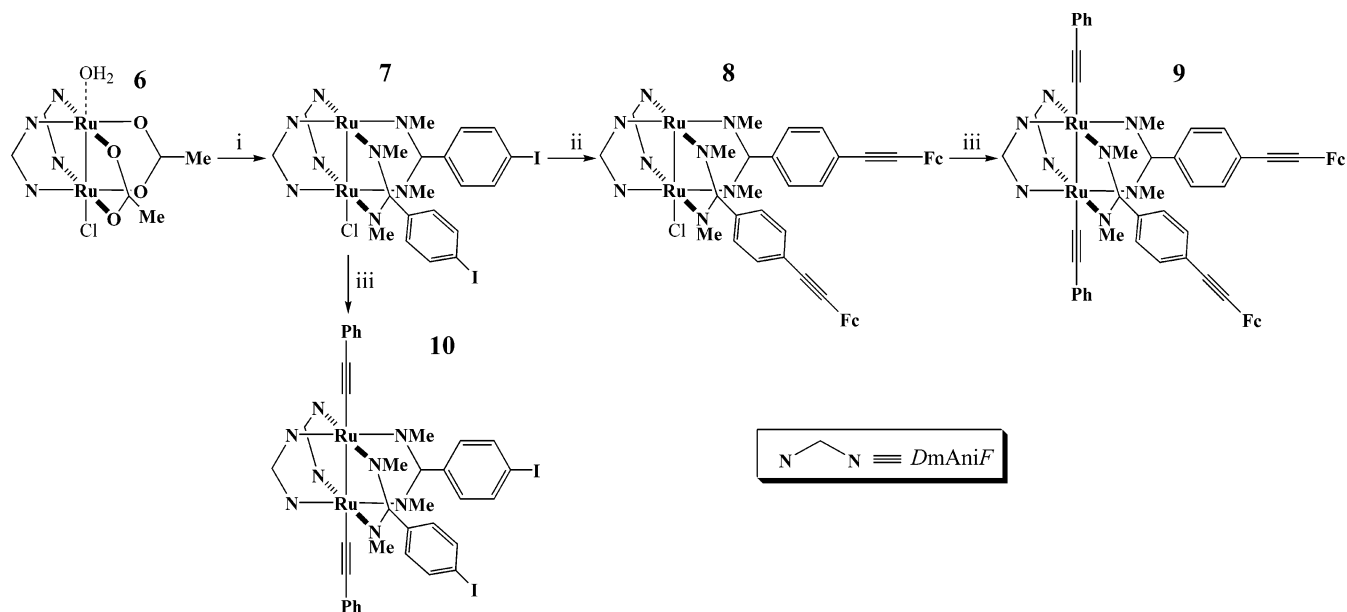
(27) (a) Angaridis, P.; Cotton, F. A.; Murillo, C. A.; Villagran, D.; Wang, X. P. *Inorg. Chem.* **2004**, *43*, 8290. (b) Angaridis, P.; Berry, J. F.; Cotton, F. A.; Lei, P.; Lin, C.; Murillo, C. A.; Villagran, D. *Inorg. Chem. Commun.* **2004**, *7*, 9. (c) Angaridis, P.; Berry, J. F.; Cotton, F. A.; Murillo, C. A.; Wang, X. P. *J. Am. Chem. Soc.* **2003**, *125*, 10327.

(28) Chen, W.-Z.; Ren, T. *Organometallics* **2004**, *23*, 3766.

(29) Brandsma, L. *Preparative Acetylenic Chemistry*; Elsevier: Amsterdam, 1988.

Scheme 1. Synthesis of Ru₂(LL)₃(LL') Type Compounds^a

^a (i) 2 equiv *N,N'*-dimethyl-4-iodobenzamidine, LiCl, Et₃N; 79%. (ii) HC₂Y, *trans*-Pd(PPh₃)₂Cl₂, CuI, ⁱPr₂NH, THF, rt; **3a**: 41%, **3b**: 49%. (iii) Bu₄NF, THF; 57%. (iv) 3 equiv LiC₄TMS, THF; **4a**: 43%, **4b**: 37%, **5**: 46%. (v) HC₂SiⁱPr₃, *trans*-Pd(PPh₃)₂Cl₂, CuI, ⁱPr₂NH, THF, rt.

Scheme 2. Synthesis of Ru₂(LL)₂(LL')₂ Type Compounds^a

^a (i) 4 equiv *N,N'*-dimethyl-4-iodobenzamidine, LiCl, Et₃N; 75%. (ii) HC₂Fc, Pd(PPh₃)₂Cl₂, CuI, ⁱPr₂NH, THF, rt; 52%. (iii) 8 equiv LiC₂Ph, THF, **9**: 46%, **10**: 51%.

treating **2** with terminal alkyne HC≡CY under Sonogashira conditions furnished compounds Ru₂(DmAniF)₃-(DMBA-4-C₂Y)Cl (Y = SiⁱPr₃ (**3a**) and Fc (**3b**)), and treating **7** with HC≡CFc yielded *cis*-Ru₂(DmAniF)₂-(DMBA-4-C₂Fc)₂Cl (**8**), all in good yields. Compounds **3a/3b** reacted with 3 equiv of LiC₄SiMe₃ to yield *trans*-bis(butadiynyl) compounds **4a/4b** under conditions analogous to that established early for diruthenium compounds.²¹ Similarly, compound **8** reacted with 8 equiv of LiC≡CPh to yield compound **9**. In an attempt to explore alternative routes to compounds **4**, compound **2** reacted with LiC₄SiMe₃ in excess to yield axial bis-butadiynyl adduct **5**. The ensuing cross-coupling reac-

tion under Sonogashira conditions, however, did not produce the desired product due to the dissociation of axial butadiynyls under the experimental conditions (see Supporting Information).

All monochloro compounds, namely, **1**, **2**, **3a/3b**, **6**, **7**, and **8**, are Ru₂(II,III) species and paramagnetic, with μ_{eff} ranging from 3.60 to 3.87 μ_{B} , which is consistent with a *S* = 3/2 ground state typical for Ru₂(DArF)₄Cl type compounds.³¹ On the other hand, all axial bis-alkynyl compounds **4a/4b**, **5**, **9**, and **10** are Ru₂(III,III) species and diamagnetic, the latter of which enables the attainment of well-resolved ¹H NMR spectra. These axial bis-alkynyl compounds also retain the feature of vis-NIR chromophores with an intense peak at ca. 520 nm

(30) *Metal-catalyzed Cross Coupling Reactions*; Diederich, F., Stang, P. J., Eds.; Wiley-VCH: Weinheim, 1998.

(31) Cotton, F. A.; Ren, T. *Inorg. Chem.* **1995**, *34*, 3190.

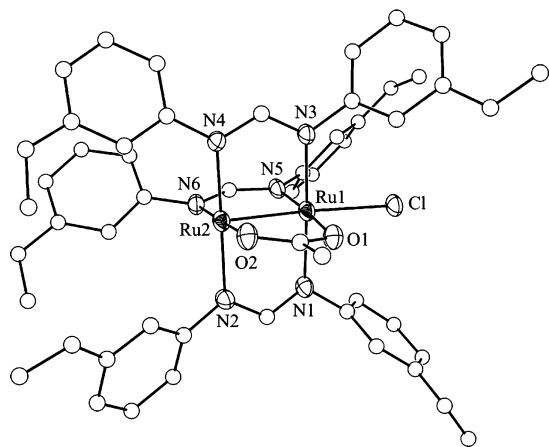


Figure 1. ORTEP representation of molecule **1** at 30% probability level.

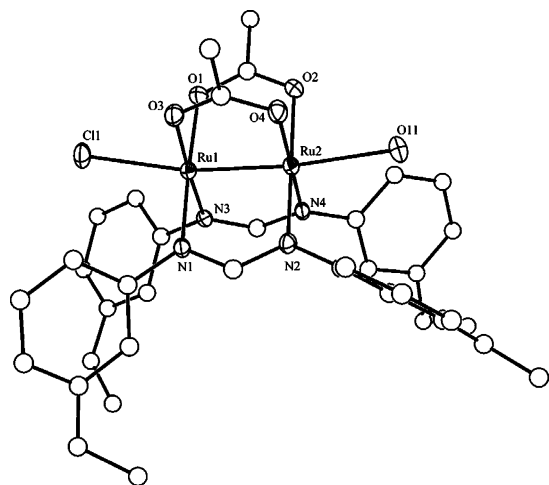


Figure 2. ORTEP representation of molecule **6** at 30% probability level.

and a significant peak at 910 nm. Vis–NIR spectra for all compounds are provided in the Supporting Information.

Molecular Structures. The structures of **1**, **4a**, **5**, **6**, **9**, and **10** were determined through single-crystal X-ray diffraction studies, and the ORTEP plots are shown in Figures 1–6. The selected bond lengths and angles for compounds **1**, **4a**, and **5** are listed in Table 1, while those of **6**, **9**, and **10** are in Table 2. It is clear that the paddlewheel arrangement of the bridging ligands around the Ru₂ core is adopted in all compounds. In particular, structural studies of compounds **9** and **10** confirmed that the *cisoid* arrangement of two sets of bridging ligands initially determined for **6** is retained, indicating the absence of structural rearrangement under both the ligand substitution and cross-coupling reaction conditions.

The Ru–Ru bond lengths for compounds **1** and **6** are 2.3220(7) and 2.3219(4) Å, respectively, which are between those reported for the chloro compounds of Ru₂⁵⁺ tetracarboxylate (2.27–2.30 Å) and tetraformamidate (2.34–2.39 Å) species.³² For **1**, the average of the Ru–O_{eq} bond lengths is 2.079[5] Å, which is slightly longer than the average Ru–N_{eq} distance of 2.064[5] Å. The contrast is more significant in **6**: the average Ru–

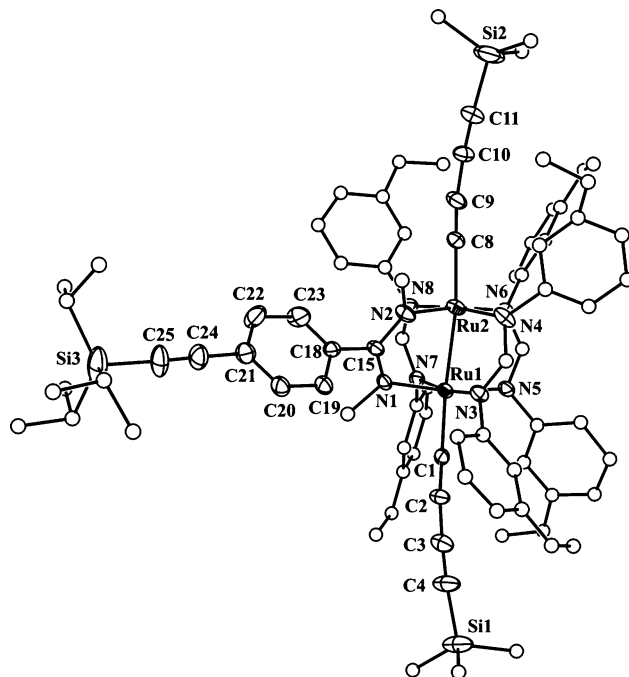


Figure 3. ORTEP representation of molecule **4a** at 20% probability level.

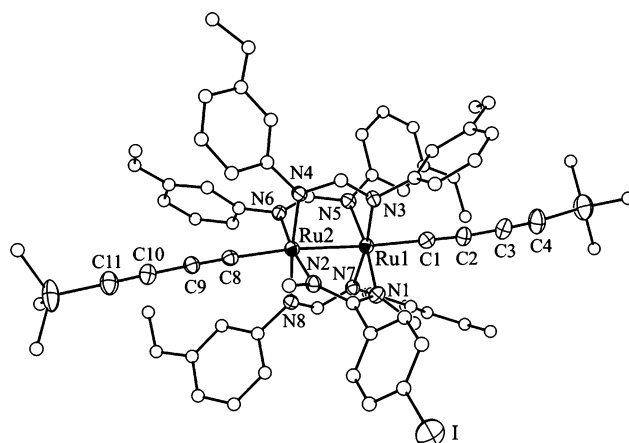


Figure 4. ORTEP representation of molecule **5** at 30% probability level.

O_{eq} distance is 2.076[3] Å and the average Ru–N_{eq} distance is 2.036[3] Å. While compound **1** contains only an axial chloro ligand, compound **6** has one H₂O molecule occupying the remaining axial position.

As can be seen from Figures 3–6 and Tables 1–2, all bis-alkynyl compounds **4a**, **5**, **9**, and **10** display similar coordination geometry around the Ru₂ core. The Ru–Ru bond lengths, 2.5467(7), 2.5581(5), 2.5069(4), and 2.4977(6) Å, for **4a**, **5**, **9**, and **10**, respectively, are significantly longer than those of **1** and **6**, reflecting the loss of the σ (Ru–Ru) bond upon the formation of two σ (Ru–C) bonds.²⁰ It is interesting to note that the Ru–Ru bond lengths determined for **4a** and **5** are close to the average between that of Ru₂(DmAniF)₄(C₄SiMe₃)₂ (2.5990(3) Å)^{20d} and Ru₂(DMBA)₄(C₄H)₂ (2.4559(6) Å).^{20g} The observed variation can be rationalized on the basis of the electron density on the Ru₂ core that is determined by the donor ability of the bridging ligand: the most donating DMBA resulted in the shortest bond length, the least donating DmAniF resulted in the longest, and the combination of both type ligands (**4a**

(32) Cotton, F. A.; Walton, R. A. *Multiple Bonds Between Metal Atoms*; Oxford University Press: Oxford, 1993.

Table 1. Selected Bond Lengths (Å) and Angles (deg) for Compounds 1, 4a, and 5

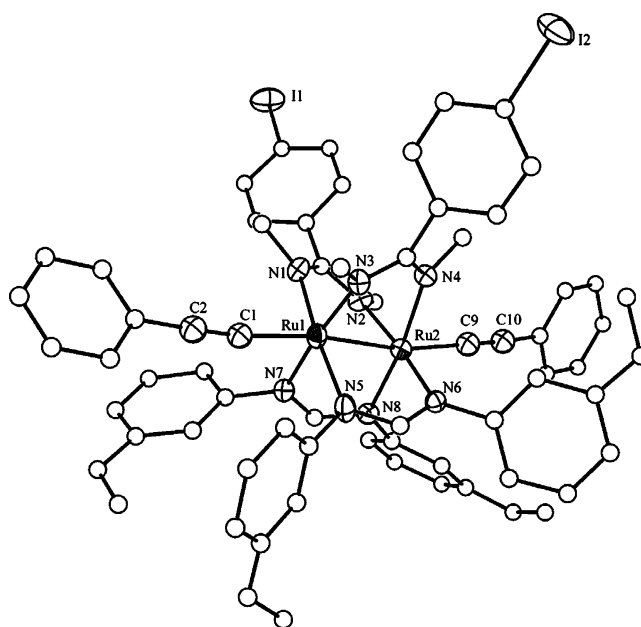
1		4a		5	
Ru1–Ru2	2.3220(7)	Ru1–Ru2	2.5467(7)	Ru1–Ru2	2.5581(5)
Ru1–N1	2.088(5)	Ru1–C1	1.976(6)	Ru1–C1	1.949(5)
Ru1–N3	2.103(5)	Ru2–C8	1.988(7)	Ru2–C8	1.954(5)
Ru1–N5	2.068(6)	Ru1–N1	2.038(1)	Ru1–N1	2.063(3)
Ru2–N2	2.049(5)	Ru1–N3	2.126(5)	Ru1–N3	2.101(4)
Ru2–N4	2.063(5)	Ru1–N5	2.054(4)	Ru1–N5	2.049(3)
Ru2–N6	2.013(6)	Ru1–N7	2.013(5)	Ru1–N7	2.000(4)
Ru1–O1	2.082(5)	Ru2–N2	2.013(4)	Ru2–N2	1.971(3)
Ru2–O2	2.075(5)	Ru2–N4	1.999(5)	Ru2–N4	2.005(3)
Ru1–Cl	2.405(2)	Ru2–N6	2.054(5)	Ru2–N6	2.110(3)
		Ru2–N8	2.118(5)	Ru2–N8	2.101(4)
		C1–C2	1.193(8)	C1–C2	1.214(6)
		C2–C3	1.38(1)	C2–C3	1.387(7)
		C3–C4	1.208(9)	C3–C4	1.189(7)
		C8–C9	1.177(9)	C8–C9	1.206(6)
		C9–C10	1.379(10)	C9–C10	1.379(6)
		C10–C11	1.180(9)	C10–C11	1.208(6)
		C24–C25	1.172(8)		
Ru2–Ru1–Cl	175.37(5)	Ru1–Ru2–C8	166.8(2)	Ru1–Ru2–C8	163.9(1)
		C1–Ru1–Ru2	163.0(2)	C1–Ru1–Ru2	162.2(1)
		C1–C2–C3	172.9(7)	C1–C2–C3	172.7(5)
		C2–C3–C4	176.3(9)	C2–C3–C4	177.5(6)
		C8–C9–C10	172.1(8)	C8–C9–C10	176.1(5)
		C11–C10–C9	175.0(9)	C11–C10–C9	178.4(5)

Table 2. Selected Bond Lengths (Å) and Angles (deg) for Compounds 6, 9, and 10

6		9		10	
Ru1–Ru2	2.3219(4)	Ru1–Ru2	2.5069(4)	Ru1–Ru2	2.4977(6)
Ru1–N1	2.050(3)	Ru1–C1	1.973(5)	Ru1–C1	1.975(5)
Ru1–N3	2.033(3)	Ru2–C9	1.974(4)	Ru2–C9	1.966(6)
Ru2–N2	2.026(3)	Ru1–N1	2.070(3)	Ru1–N1	2.026(4)
Ru2–N4	2.032(3)	Ru1–N3	1.972(3)	Ru1–N3	1.987(4)
Ru1–O1	2.085(3)	Ru1–N5	2.043(3)	Ru1–N5	2.065(4)
Ru1–O3	2.080(2)	Ru1–N7	2.116(4)	Ru1–N7	2.122(4)
Ru2–O2	2.065(3)	Ru2–N2	1.979(3)	Ru2–N2	2.035(4)
Ru2–O4	2.075(2)	Ru2–N4	2.088(3)	Ru2–N4	2.083(4)
Ru2–O11	2.466(3)	Ru2–N6	2.115(3)	Ru2–N6	2.071(4)
Ru1–Cl	2.457(1)	Ru2–N8	2.038(4)	Ru2–N8	2.027(4)
		C1–C2	1.203(6)	C1–C2	1.187(7)
		C9–C10	1.210(6)	C9–C10	1.210(7)
		C26–C27	1.195(6)		
		C47–C48	1.181(7)		
Ru2–Ru1–Cl	169.49(3)	Ru1–Ru2–C9	162.5(1)	Ru1–Ru2–C9	168.3(2)
Ru1–Ru2–O11	168.40(7)	C1–Ru1–Ru2	161.6(1)	C1–Ru1–Ru2	169.1(2)

and **5**) gave intermediate values. In the same vein, the observed Ru–Ru bond lengths for the phenylethynyl adducts (**9** and **10**) are shorter than those for the butadiynyl adducts (**4a** and **5**), since phenylethynyl is a stronger donor than butadiynyl. In the case of **4a**, the ethynyl unit on the DMBA ligand is orthogonal to the bis(butadiynyl) on the axial positions. There are also significant deviations from linearity in Ru–Ru–C1 (163.0(2)°) and Ru–Ru–C8 (166.8(2)°) angles, which are attributed to a second-order Jahn–Teller effect common to Ru₂(III,III)-alkynyl compounds.^{20,21}

Structural features of compound **9** are worthy of mention because of the use of ferrocenyl as peripheral substituents. The C–C bond lengths of two ferrocenylethynyl moieties are 1.195(6) (C26–C27) and 1.181(7) Å (C47–C48), which agree with the expected value of 1.20 Å within experimental error. Interestingly, the unique axis of both ferrocenyl groups, i.e., the vector defined by linking the centroid of Cp rings and the Fe center (shown as a dashed line in Figure 6), parallels the Ru₂–acetylide linkage. The distance between Fe1 and Fe2 centers is 18.528 Å. Previously, a series of Ru₂^{II,III}(O₂CY)₄ type compounds with Y as (CH₂)_nFc (*n* = 0–2), (CH₂)₂Fc, and Rc (ruthenocenyl) were reported

**Figure 5.** ORTEP representation of molecule **10** at 30% probability level.

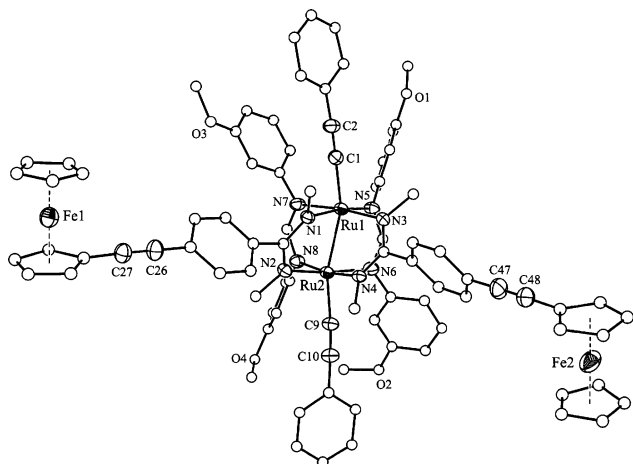


Figure 6. ORTEP representation of molecule **9** at 30% probability level. All carbon atoms except the acetylene are shown as unlabeled isotropic open circles for clarity.

by Aquino, where the unique axes of metallacenes are orthogonal to the Ru–Ru vector in all three structurally characterized compounds.³³ The contrast in the alignment between ours and Aquino's compounds likely originates from the subtle difference in lattice packing: the peripheral Fc/Rc units in $\text{Ru}_2^{\text{II,III}}(\text{O}_2\text{CY})_4$ type compounds are close enough to the Ru–Ru vector that they can fill the void between adjacent bridging ligands by being orthogonal to the Ru–Ru vector. On the other hand, the Fc units in **9** are too far away from the Ru–Ru vector and the void between adjacent bridging ligands have to be filled by groups from neighboring molecules instead.

Electrochemistry. As is common to diruthenium paddlewheel species, all compounds reported display rich and often complex redox chemistry. Cyclic voltammograms (CVs) measured for $\text{Ru}_2(\text{LL})_3(\text{LL}')$ type compounds, namely, **1**–**5**, are shown in Figure 7. Compound **1** exhibits three Ru_2 -based redox couples: a one-electron oxidation (**B**) and two one-electron reductions (**C** and **D**). The first reduction (**C**) is irreversible due to fast dissociation of the axial Cl^- ligand upon reduction (in Scheme 3), a phenomenon frequently observed in other $\text{Ru}_2(\text{LL})_4\text{Cl}$ type compounds.^{19,34} The resultant species, $\text{Ru}_2(\text{DmAniF})_3(\text{OAc})$, is reoxidized at a more positive potential (**E**). Unsurprisingly, these characteristics are almost identical to that reported for $\text{Ru}_2(\text{DpAniF})_3(\text{OAc})\text{Cl}$,²⁷ although the electrode potentials for $\text{Ru}_2(\text{DpAniF})_3(\text{OAc})\text{Cl}$ are slightly shifted in the cathodic direction since 4-MeO is a more electron-donating substituent than 3-MeO. While the CVs of compounds **2** and **3** are quite similar to that of **1**, the electrode potentials of corresponding couples have been cathodically shifted by at least 100 mV, reflecting the fact that DMBA is a much stronger donor than acetate.

Cyclic voltammograms of bis(butadiynyl) adducts **4a** and **5** feature one irreversible oxidation (**A**) and two reversible one-electron reductions (**B** and **C**), and the reversibility of the latter reflects the robustness of Ru–C

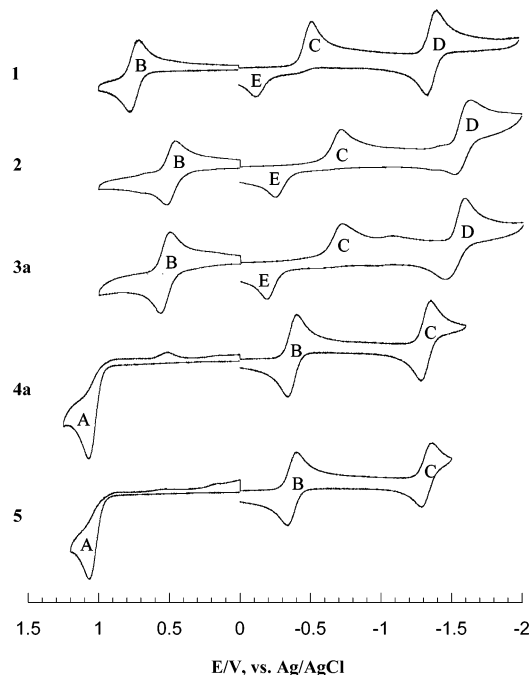


Figure 7. Cyclic voltammograms of $\text{Ru}_2(\text{DmAniF})_3(\text{OAc})$ and $\text{Ru}_2(\text{DmAniF})_3(\text{DMBA})$ type compounds recorded in a 0.20 M THF solution of Bu_4NPF_6 at a scan rate of 0.10 V/s.

Scheme 3. Assignments of Observed Ru_2 -Based Redox Couples; X Stands for Axial Ligand

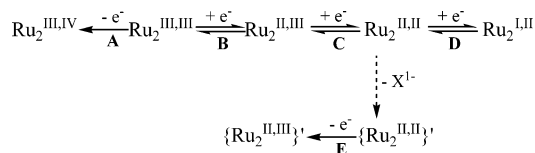


Table 3. Electrode Potentials (V) of **4a, **5**, and Related Compounds**

	$E_{\text{pa}}(\text{A})$	$E_{1/2}(\text{B})$	$E_{1/2}(\text{C})$
$\text{Ru}_2(\text{DmAniF})_4(\text{C}_4\text{SiMe}_3)_2$	1.17	−0.32	−1.32
5	1.06	−0.37	−1.32
4a	1.06	−0.39	−1.39
$\text{Ru}_2(\text{DMBA})_4(\text{C}_4\text{SiMe}_3)_2$	0.73	−0.90	−1.94

bonds upon reduction. The electrode potentials of compounds **4a** and **5** are listed in Table 3 along with those for $\text{Ru}_2(\text{DmAniF})_4(\text{C}_4\text{SiMe}_3)_2$ and $\text{Ru}_2(\text{DMBA})_4(\text{C}_4\text{SiMe}_3)_2$.²¹ Clearly, the potentials of redox couples in compounds **4a** and **5** are slightly more negative than those of the corresponding couples in $\text{Ru}_2(\text{DmAniF})_4(\text{C}_4\text{SiMe}_3)_2$, but far more positive than those in $\text{Ru}_2(\text{DMBA})_4(\text{C}_4\text{SiMe}_3)_2$. The variation among redox potentials is easily explained by the fact that DMBA is a much stronger donor than *DARF* ligands. Furthermore, compounds **4a** and **5** are very similar to $\text{Ru}_2(\text{DmAniF})_4(\text{C}_4\text{SiMe}_3)_2$ in terms of the reversibility of their redox couples.

Cyclic voltammograms (CVs) measured for several $\text{Ru}_2(\text{LL})_2(\text{LL}')_2$ type compounds, namely, **6**, **7**, and **10**, are shown in Figure 8. $\text{Ru}_2(\text{DmAniF})_2(\text{OAc})_2\text{Cl}$ (**6**) displays three Ru_2 -based couples similar to that of **1**, but at more anodic potentials. The increased electron deficiency at the Ru_2 core is also reflected by the irreversibility of couple **B**. $\text{Ru}_2(\text{DpAniF})_2(\text{OAc})_2\text{Cl}$, the more electron-rich analogue reported by Cotton et al., exhibited a reversible **B**.²⁷ Upon the formation of **7** via

(33) (a) Cooke, M. W.; Cameron, T. S.; Robertson, K. N.; Swarts, J. C.; Aquino, M. A. S. *Organometallics* **2002**, *21*, 5962. (b) Cooke, M. W.; Murphy, C. A.; Cameron, T. S.; Swarts, J. C.; Aquino, M. A. S. *Inorg. Chem. Commun.* **2000**, *3*, 721.

(34) Lin, C.; Ren, T.; Valente, E. J.; Zubkowsky, J. D.; Smith, E. T. *Chem. Lett.* **1997**, 753.

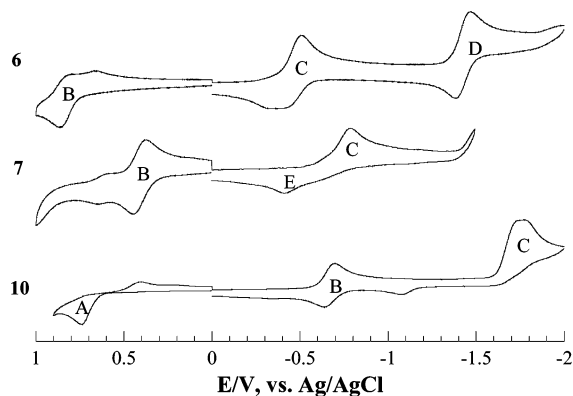


Figure 8. Cyclic voltammograms of $\text{Ru}_2(\text{LL})_2(\text{LL}')_2$ type compounds **6**, **7**, and **10**.

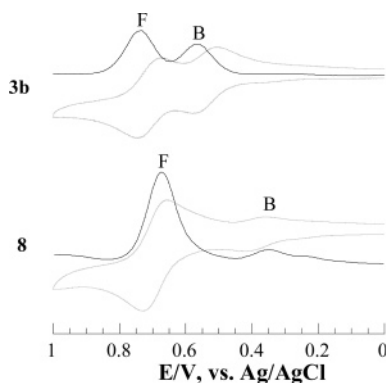


Figure 9. Differential pulse (solid) and cyclic (gray) voltammograms of compounds **3b** and **8**.

the replacement of acetate by DMBA-I, the oxidation couple **B** is shifted by -0.33 V, reflecting the extraordinary donor strength of DMBA ligands. Compound **7**, however, is quite unstable toward reduction. The CV of the bis-phenylethynyl derivative **10** is quasi-reversible on the first reduction **B**, but irreversible on oxidation (**A**) and second reduction (**C**). Clearly, $\text{Ru}_2(\text{LL})_2(\text{LL}')_2$ type compounds are less redox-robust than $\text{Ru}_2(\text{LL})_3(\text{LL}')$ type compounds, although the origin of the instability is not presently obvious.

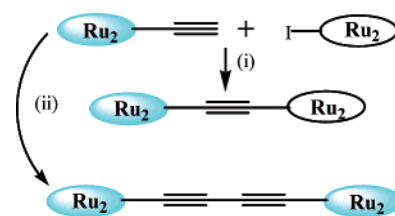
CVs of $\text{Ru}_2(\text{DmAniF})_{4-n}(\text{DMBA-4-C}_2\text{Fc})_n$ ($n = 1$ and 2) type compounds, i.e., **3b**, **4b**, **8**, and **9**, generally resemble those of the corresponding $\text{Ru}_2(\text{DmAniF})_{4-n}(\text{DMBA-4-I})_n$ compounds and are all provided in the Supporting Information. The existence of two Fc groups within a single molecule in both **8** and **9** presents a unique opportunity to gauge the intramolecular electronic coupling between two Fc centers. For this reason, both the CVs and DPVs of $\text{Ru}_2(\text{DmAniF})_3(\text{DMBA-4-C}_2\text{Fc})\text{Cl}$ (**3b**) and $\text{Ru}_2(\text{DmAniF})_2(\text{DMBA-4-C}_2\text{Fc})_2\text{Cl}$ (**8**) in the anodic region (0 to 1.0 V versus Ag/AgCl) are shown in Figure 9. Voltammograms of both compounds feature the Fc-centered oxidation (**F**) in addition to the Ru_2 -based oxidation (**B**). It is immediately clear from comparing **8** with **3b** that two Fc centers in **8** are oxidized simultaneously and, hence, are not electronically coupled. Previously, Aquino et al. reported a 40 mV separation between two Fc-centered 2-e^- oxidations for $[\text{Ru}_2(\text{O}_2\text{C}(\text{CH}_2)_2\text{Fc})_4](\text{PF}_6)$, which was attributed to a weak intramolecular electronic coupling.³³ However, the absence of coupling in **8** is not surprising, considering that two Fc units are separated by 18 bonds in **8** and only 10 bonds in $[\text{Ru}_2(\text{O}_2\text{C}(\text{CH}_2)_2\text{Fc})_4](\text{PF}_6)$. On the other

hand, our studies of the $\text{trans-Fc}(\text{CC})_{2n}[\text{Ru}_2(\text{DMBA})_4](\text{CC})_{2n}\text{Fc}$ ($n = 1$ and 2) family provide unambiguous evidence of *strong* couplings between two Fc groups separated by up to 11 bonds.²⁴ It appears that the charge transfer along the axial direction of diruthenium paddlewheel species is far more facile than that along the equatorial direction.

Conclusions

We presented methods for preparing $\text{Ru}_2(\text{DmAniF})_{4-n}(\text{OAc})_n\text{Cl}$ ($n = 1$ and 2) in excellent yields, which complement the routes developed by Cotton and Jiménez-Aparicio.^{26,27} Further derivatization yielding $\text{Ru}_2(\text{DmAniF})_{4-n}(\text{DMBA-I})_n\text{Cl}$ was also demonstrated, and the resultant compounds became a *springboard* for peripheral functionalization of Ru_2 species through Pd-catalyzed cross-coupling reactions. The iodo- and alkynyl-functionalized diruthenium complexes are of interest as building blocks for both homo- and heterodimeric supermolecular molecules, as shown in Scheme 4. Many interesting supramolecules have been self-assembled from dimetallic units linked by ditopic ligands at the equatorial positions in recent years.^{35,36} Most of the resultant architectures are centrosymmetric due to the extensive use of symmetric ditopic linkers. Heterodimeric assembly outlined in Scheme 4, on the other hand, may lead to supramolecules of energy gradient or as bulk polar materials. In addition, the presence of the peripheral ethyne functionality should enable the formation of diruthenium conjugates with biomolecules through *click* reactions.³⁷ These aspects are being vigorously pursued in our laboratory.

Scheme 4. Hetero- and Homodimeric Diruthenium Supramolecules through (i) Sonogashira Coupling and (ii) Glaser Coupling



Experimental Section

Copper(I) iodide and phenylacetylene were purchased from Acros, 1,4-bis(trimethylsilyl)-1,3-butadiyne and triisopropylsilylacetylene were purchased from GFS Chemicals, silica gel was purchased from Merck, and *trans*-Pd(PPh₃)₂Cl₂ was

(35) (a) Cotton, F. A.; Lin, C.; Murillo, C. A. *Acc. Chem. Res.* **2001**, *34*, 759. (b) Cotton, F. A.; Lin, C.; Murillo, C. A. *Proc. Nat. Acad. Sci., U.S.A.* **2002**, *99*, 4810. (c) Chisholm, M. H. *J. Chem. Soc., Dalton Trans.* **2003**, 3821.

(36) (a) Cotton, F. A.; Liu, C. Y.; Murrilo, C. A.; Villagran, D.; Wang, X. P. *J. Am. Chem. Soc.* **2004**, *126*, 14822. (b) Cotton, F. A.; Donahue, J. P.; Lin, C.; Murillo, C. A. *Inorg. Chem.* **2001**, *40*, 1234. (c) Bera, J. K.; Angaridis, P.; Cotton, F. A.; Petrukhina, M. A.; Fanwick, P. E.; Walton, R. A. *J. Am. Chem. Soc.* **2001**, *123*, 1515. (d) Kuang, S.-M.; Fanwick, P. E.; Walton, R. A. *Inorg. Chem.* **2002**, *41*, 405. (e) Bursten, B. E.; Chisholm, M. H.; Clark, R. J. H.; Firth, S.; Hadad, C. M.; MacIntosh, A. M.; Wilson, P. J.; Woodward, P. M.; Zaleski, J. M. *J. Am. Chem. Soc.* **2002**, *124*, 3050. (f) Bursten, B. E.; Chisholm, M. H.; Clark, R. J. H.; Firth, S.; Hadad, C. M.; Wilson, P. J.; Woodward, P. M.; Zaleski, J. M. *J. Am. Chem. Soc.* **2002**, *124*, 12244.

(37) (a) Kolb, H. C.; Finn, M. G.; Sharpless, K. B. *Angew. Chem., Int. Ed.* **2001**, *40*, 2004. (b) Kolb, H. C.; Sharpless, K. B. *Drug Discovery Today* **2003**, *8*, 1128.

purchased from Strem Chemicals. Ferrocenylacetylene was prepared according to the literature.³⁸ ¹H NMR spectra were recorded on a Bruker AVANCE300 NMR spectrometer, with chemical shifts (δ) referenced to the residual CHCl₃. Visible–near-infrared spectra in THF were obtained with a Perkin-Elmer Lambda-900 UV–vis–NIR spectrophotometer. Magnetic susceptibility was measured at 294 K with a Johnson Matthey Mark-I magnetic susceptibility balance. Elemental analysis was performed by Atlantic Microlab, Norcross, GA. Cyclic and differential pulse voltammograms were recorded in 0.2 M (*n*-Bu)₄NPF₆ solution (THF, N₂-degassed) on a CHI620A voltammetric analyzer with a glassy carbon working electrode (diameter = 2 mm), a Pt-wire auxiliary electrode, and a Ag/AgCl reference electrode. The concentration of diruthenium species was always 1.0 mM. The ferrocenium/ferrocene couple was observed at 0.582 V (vs Ag/AgCl) under the experimental conditions.

Preparation of Ru₂(DmAniF)₃(OAc)Cl (1). A round-bottom flask was charged with Ru₂(OAc)₄Cl (1.0 g, 2.11 mmol), *N,N'*-di(*m*-methoxyphenyl)formamidine (1.58 g, 6.33 mmol), LiCl (0.50 g), Et₃N (2 mL), and 40 mL of THF. The mixture was gently refluxed for 12 h. The color changed to dark purple. The reaction mixture was then filtered through a short silica gel pad (2 cm). Further purification with silica column (eluent: ethyl acetate/hexanes = 1/2 to 1/1) yielded **1** as a purple crystalline material (1.95 g, 87% based on Ru). Data for **1**: *R*_f(ethyl acetate/hexanes = 1/1), 0.45. MS-FAB (*m/e*, based on ¹⁰¹Ru): 1028 [M⁺ – Cl]. Vis–NIR, λ_{\max} (nm, ϵ (M⁻¹ cm⁻¹)): 526(3860). Anal. for C₄₇H₄₈ClN₆O₈Ru₂·THF, found(calcd): C, 53.92(53.99); H, 4.89(4.97); N, 7.46(7.41). χ_{mol} (corrected) = 5.80 × 10⁻³ emu, μ_{eff} = 3.72 μ_{B} . Cyclic voltammogram [*E*_{1/2}/V, $\Delta E_{\text{p}}/V$, *i*_{backward}/*i*_{forward}]: **B**, 0.743, 0.064, 0.88; **D**, -1.382, 0.062, 0.98; *E*_{pc}(**C**), -0.525 V; *E*_{pa}(**E**), -0.120 V.

Preparation of Ru₂(DmAniF)₃(DMBA-I)Cl (2). A mixture of **1** (1.0 g, 0.94 mmol), *N,N'*-dimethyl-4-iodobenzamidine (0.52 g, 1.88 mmol), LiCl (0.20 g), Et₃N, (2 mL) and THF (40 mL) was refluxed overnight, with the color of the reaction mixture changing from dark purple to green. The reaction mixture was filtered through silica gel. After solvent removal, the residue was purified with a silica column (ethyl acetate/hexanes/triethylamine = 5/10/1) to yield **2** as a green microcrystalline material (0.95 g, 79%). Data for **2**: *R*_f(ethyl acetate/hexanes/triethylamine, v/v/v: 5/10/1), 0.35. MS-FAB (*m/e*, based on ¹⁰¹Ru): 1242 [M⁺ – Cl]. Vis–NIR, λ_{\max} (nm, ϵ (M⁻¹ cm⁻¹)): 468(2310). Anal. for C₅₄H₅₅ClN₈O₆IRu₂·Et₃N, found(calcd): C, 52.63(52.31); H, 4.88(5.12); N, 8.83(9.14). χ_{mol} (corrected) = 5.56 × 10⁻³ emu, μ_{eff} = 3.64 μ_{B} . Cyclic voltammogram [*E*_{1/2}/V, $\Delta E_{\text{p}}/V$, *i*_{backward}/*i*_{forward}]: **B**, 0.551, 0.063, 0.78; **D**, -1.530, 0.093, 0.61; *E*_{pc}(**C**), -0.669 V; *E*_{pa}(**E**), -0.200 V.

Preparation of Ru₂(DmAniF)₃(DMBA-4-C₂SiⁱPr₃)Cl (3a). A mixture of **2** (1.0 g, 0.78 mmol), *trans*-Pd(PPh₃)₂Cl₂ (0.2 g, 0.28 mmol), CuI (0.10 g, 0.52 mmol), ⁱPr₂NH (20 mL), THF (20 mL), and trisopropylsilylacetylene (0.5 mL) was stirred at room temperature overnight. After the removal of solvent, the residue was purified with a silica column (ethyl acetate/hexane/triethylamine = 3/9/1) to afford **3a** as a green microcrystalline material (0.43 g, 41%). Data for **3a**: *R*_f(ethyl acetate/hexane/triethylamine = 3/9/1), 0.28. MS-FAB (*m/e*, based on ¹⁰¹Ru): 1296 [M⁺ – Cl]. Vis–NIR, λ_{\max} (nm, ϵ (M⁻¹ cm⁻¹)): 467(3730). Anal. for C₆₅H₇₆ClN₈O₆Ru₂Si·THF, found(calcd): C, 59.14(59.06); H, 6.03(6.03); N, 8.17(7.99). χ_{mol} (corrected) = 5.47 × 10⁻³ emu, μ_{eff} = 3.60 μ_{B} . Cyclic voltammogram [*E*_{1/2}/V, $\Delta E_{\text{p}}/V$, *i*_{backward}/*i*_{forward}]: **B**, 0.565, 0.059, 0.83; **D**, -1.494, 0.109, 0.83; *E*_{pc}(**C**), -0.671 V; *E*_{pa}(**E**), -0.178 V.

Preparation of Ru₂(DmAniF)₃(DMBA-4-C₂Fc)Cl (3b). A mixture of **2a** (1.06 g, 0.83 mmol), ferrocenylacetylene (0.21 g, 1.00 mmol), *trans*-Pd(PPh₃)₂Cl₂ (0.30 g, 0.42 mmol), CuI (0.15 g, 0.79 mmol), ⁱPr₂NH (20 mL), and THF (20 mL) was stirred

at room temperature overnight. After the removal of solvent, the residue was purified with a silica column (ethyl acetate/hexane/triethylamine = 3/6/1) to afford **3b** as a green microcrystalline material. Yield: 0.55 g, 49%. Data for **3b**: *R*_f(ethyl acetate/hexane/triethylamine = 3/6/1), 0.46. MS-FAB (*m/e*, based on ¹⁰¹Ru): 1324 [M⁺ – Cl]. Anal. for C₆₆H₆₄ClN₈O₆Ru₂·Fe·THF, found(calcd): C, 59.10(58.76); H, 5.34(5.07); N, 8.24(7.83). Vis–NIR, λ_{\max} (nm, ϵ (M⁻¹ cm⁻¹)): 464(3760). χ_{mol} (corrected) = 5.29 × 10⁻³ emu, μ_{eff} = 3.56 μ_{B} . Cyclic voltammogram [*E*_{1/2}/V, $\Delta E_{\text{p}}/V$, *i*_{backward}/*i*_{forward}]: **F**, 0.542, 0.073, 0.87; **B**, 0.711, 0.066, 0.57; *E*_{pc}(**C**), -0.733 V; *E*_{pa}(**E**), -0.173 V.

Preparation of Ru₂(DmAniF)₃(DMBA-4-C₂H)Cl (3c). To **3a** (0.20 g, 0.15 mmol) dissolved in 30 mL of THF was added 0.5 mL of TBAF (tetrabutylammonium fluoride, 1 M in THF), and the mixture was stirred for ca. 20 min before being filtered through a 2 cm silica gel pad deactivated with Et₃N. After the solvent removal, the residue was purified with chromatography (THF/hexanes/Et₃N = 3/9/1) to yield 0.10 g of a green microcrystalline material (57%). Anal. for C₅₆H₅₆ClN₈O₆Ru₂·1.5C₆H₁₄, found(calcd): C, 59.83 (60.63); H, 6.02(6.29); N, 8.59(8.32).

Preparation of Ru₂(DmAniF)₃(DMBA-4-C₂SiⁱPr₃)(C₄-SiMe₃)₂ (4a). To a 20 mL THF solution containing 0.9 mmol of Me₃SiC₄SiMe₃ was added 0.9 mL of BuLi (1.0 M in hexanes) at about -80 °C. The mixture was slowly warmed to room temperature and stirred for another 1 h to yield a slightly yellow solution. The solution was added to 40 mL of THF solution containing **3a** (0.30 mmol, 0.4 g) at room temperature, and the mixture was stirred for 2 h, during which the solution became dark red. After the solvent removal, the residue was purified with chromatography (ethyl acetate/hexanes = 1/6) to yield 0.20 g of a red powder (43%). Data for **4a**: *R*_f(ethyl acetate/hexanes = 1/6), 0.52. MS-FAB (*m/e*, based on ¹⁰¹Ru): 1539 [M⁺]. Vis–NIR, λ_{\max} (nm, ϵ (M⁻¹ cm⁻¹)): 537(13 210), 911(1250). ¹H NMR: 8.22 (s, 2H, NCHN), 7.93 (s, 2H, NCHN), 7.62–7.60 (d, 2H, aromatic), 7.19–7.08 (m, 6H, aromatic), 7.05–7.04 (d, 2H, aromatic), 6.82 (s, 2H, aromatic), 6.78 (s, 4H, aromatic), 6.69–6.68 (d, 6H, aromatic), 6.22–6.21 (d, 4H, aromatic), 6.17–6.13 (d, 2H, aromatic), 3.66 (s, 12H, OCH₃), 3.63 (s, 6H, OCH₃), 3.34 (s, 6H, NCH₃), 1.13 (d, 18H, SiCH(CH₃)₃), 0.28–0.17 (m, 3H, SiCH(CH₃)₂), 0.09 (s, 18H, Si(CH₃)₃). Anal. for C₇₉H₉₄N₈O₆Ru₂Si₃·C₆H₁₄, found(calcd): C, 62.51(62.86); H, 6.68(6.70); N, 6.62(6.90). Cyclic voltammogram [*E*_{1/2}/V, $\Delta E_{\text{p}}/V$, *i*_{backward}/*i*_{forward}]: *E*_{pa}(**A**), 1.070 V; **B**, -0.372, 0.063, 0.97; **C**, -1.319, 0.062, 0.98.

Preparation of Ru₂(DmAniF)₃(DMBA-4-C₂Fc)(C₄SiMe₃)₂ (4b). To a 20 mL THF solution containing 3.8 mmol of Me₃-SiCCCSiMe₃ was added 2.3 mL of BuLi (1.6 M in hexanes) at about -80 °C. The mixture was slowly warmed to room temperature and stirred for another 1 h to yield a slightly yellow solution. The solution was added to a 40 mL THF solution containing **3b** (0.38 mmol, 0.50 g) at room temperature, and the mixture was stirred for 2 h, during which the solution became dark red. After the solvent removal, the residue was purified with chromatography (ethyl acetate/hexanes = 1/5) to yield 0.22 g of a red powder (37%). Data for **4b**: *R*_f(ethyl acetate/hexanes = 1/5), 0.68. MS-FAB (*m/e*, based on ¹⁰¹Ru): 1556 [M⁺]. Vis–NIR, λ_{\max} (nm, ϵ (M⁻¹ cm⁻¹)): 538(16 850), 922(1280). ¹H NMR: 8.11 (s, ¹H, NCHN), 7.91 (s, 2H, NCHN), 7.83–7.81 (d, 2H, aromatic), 7.12–7.03 (m, 8H, aromatic), 6.78 (s, 2H, aromatic), 6.75 (s, 4H, aromatic), 6.70–6.68 (d, 6H, aromatic), 6.22–6.20 (d, 4H, aromatic), 6.15–6.13 (d, 2H, aromatic), 4.54–4.51 (m, 2H, ferrocenyl), 4.33–4.28 (m, 7H, ferrocenyl), 3.85 (s, 12H, NCH₃), 3.83 (s, 12H, OCH₃), 3.38 (s, 6H, OCH₃), 0.10 (s, 18H, Si(CH₃)₃). Anal. for C₈₀H₈₂FeN₈O₆Ru₂Si₂, found(calcd): C, 61.53(61.37); H, 5.29(5.28); N, 7.06(7.16). Cyclic voltammogram [*E*_{1/2}/V, $\Delta E_{\text{p}}/V$, *i*_{backward}/*i*_{forward}]: **F**, 0.509, 0.066, 0.94; *E*_{pa}(**A**), 1.060; **B**, -0.390, 0.059, 0.79; **C**, -1.349, 0.081, 0.87.

(38) Doisneau, G.; Balavoine, G.; Fillebeen-Khan, T. J. *J. Organomet. Chem.* **1982**, *425*, 113.

Table 4. Crystal Data for Compounds 1, 4a, 5, 6, 9, and 10

	1·H ₂ O	4a	5	6·H ₂ O·CH ₂ Cl ₂	9·THF	10
formula	C ₄₇ H ₅₀ ClN ₆ O ₉ Ru ₂	C ₇₉ H ₉₄ N ₈ O ₆ Ru ₂ Si ₃	C ₆₈ H ₇₃ IN ₈ O ₆ Ru ₂ Si ₂	C ₃₅ H ₄₀ Cl ₃ N ₄ O ₉ Ru ₂	C ₉₂ H ₈₆ N ₈ O ₅ Ru ₂ Fe ₂	C ₁₂₈ H ₁₂₀ I ₄ N ₁₆ O ₈ Ru ₄
fw	1080.50	1538.02	1483.56	967.18	1697.53	2922.28
space group	P $\bar{1}$	P $\bar{1}$	P2 ₁ /n	P $\bar{1}$	P2 ₁ /c	P $\bar{1}$
a, Å	13.173(1)	15.375(2)	21.2595(7)	9.8249(4)	22.1088(9)	13.9277(9)
b, Å	15.358(1)	17.521(2)	10.4058(4)	12.2573(5)	17.0020(7)	20.2552(1)
c, Å	16.802(1)	18.281(3)	33.170(1)	17.0168(7)	22.1884(9)	23.247(1)
α , deg	116.426(1)	80.35(1)		109.913(1)		69.391(1)
β , deg	107.284(1)	82.95(1)	107.811(1)	90.523(1)	93.660(1)	83.568(1)
γ , deg	96.207(1)	66.348(9)		93.375(1)		89.617(1)
V, Å ³	2789.2(4)	4439(1)	6986.2(4)	1922.5(1)	8323.5(6)	6096.2(6)
Z	2	2	4	2	4	2
T, °C	27	27	27	27	27	27
λ (Mo K α), Å	0.71073	0.71073	0.71073	0.71073	0.71073	0.71073
ρ_{calc} , g cm ⁻³	1.284	1.150	1.411	1.671	1.355	1.592
μ , mm ⁻¹	0.641	0.429	0.962	1.052	0.754	1.562
R	0.0645	0.0665	0.0532	0.0326	0.0496	0.0444
wR ₂	0.1896	0.1823	0.0781	0.0710	0.1224	0.0989

Preparation of Ru₂(DmAniF)₃(DMBA-I)(C₄SiMe₃)₂ (5).

This was synthesized using the same procedure as that for 4 with 3a replaced by 2 (0.4 g, 0.313 mmol). Compound 5 was isolated as a dark red microcrystalline material (0.21 g, 46%). Data for 5: R_f (ethyl acetate/hexanes = 1/6), 0.46. MS-FAB (m/e , based on ¹⁰¹Ru): 1486 [M⁺]. Vis-NIR, λ_{max} (nm, ϵ (M⁻¹ cm⁻¹)): 539(18 450), 910(1660). Anal. for C₆₈H₇₃IN₈O₆Ru₂Si₂, found(calcd): C, 55.15(55.05); H, 5.13(4.96); N, 7.33(7.55). ¹H NMR: 8.22 (s, 1H, NCHN), 7.93 (s, 2H, NCHN), 7.87–7.86 (d, 2H, aromatic), 7.11–7.08 (m, 6H, aromatic), 7.05–6.98 (d, 2H, aromatic), 6.84 (s, 2H, aromatic), 6.73 (s, 4H, aromatic), 6.70–6.68 (d, 6H, aromatic), 6.22–6.20 (d, 4H, aromatic), 6.18–6.17 (d, 2H, aromatic), 3.32 (s, 6H, NCH₃), 3.71 (s, 12H, OCH₃), 3.66 (s, 6H, OCH₃), 0.10 (s, 18H, Si(CH₃)₃). Cyclic voltammogram: E_{pa} (A), 1.063 V; B, -0.371, 0.060, 0.92; C, -1.324, 0.076, 0.73.

Preparation of cis-Ru₂(DmAniF)₂(OAc)₂Cl (6). A round-bottom flask was charged with Ru₂(OAc)₄Cl (0.474 g, 1.0 mmol), *N,N'*-di(*m*-methoxyphenyl)formamidine (0.64 g, 2.5 mmol), Et₃N (2 mL), and 40 mL of THF. The mixture was heated at ca. 60 °C and stirred under argon for 48 h. The reaction mixture was then filtered through a short silica gel pad (2 cm). Further purification with a silica column (flush with ethyl acetate first, then collect product with acetone) yielded 6 as a green crystalline material (0.42 g, 51% based on Ru). Data for 6: R_f (CH₂Cl₂/acetone = 2/1), 0.40. MS-FAB (m/e , based on ¹⁰¹Ru): 832 [M⁺ - Cl]. Vis-NIR, λ_{max} (nm, ϵ (M⁻¹ cm⁻¹)): 567(2970), 437(2640). Anal. for C₃₄H₃₆ClN₄O₈Ru₂·0.5THF, found(calcd): C, 47.77(47.45); H, 4.61(4.53); N, 5.89-(6.15). χ_{mol} (corrected) = 6.27 × 10⁻³ emu, μ_{eff} = 3.87 μ_B . Cyclic voltammogram [$E_{1/2}$ /V, ΔE_p /V, $i_{\text{backward}}/i_{\text{forward}}$]: E_{pa} (B), 0.743; D, -1.426, 0.085, 0.93; E_{pc} (C), -0.510 V.

Preparation of cis-Ru₂(DmAniF)₂(DMBA-I)₂Cl (7). Synthesis of 7 was analogous to that of 2 with 4 equiv of *N,N'*-dimethyl-4-iodobenzamidine. Yield: 75%. R_f (ethyl acetate/hexanes = 1/2). MS-FAB (m/e , based on ¹⁰¹Ru): 1261. χ_{mol} (corrected) = 6.08 × 10⁻³ emu, μ_{eff} = 3.81 μ_B . Vis-NIR, λ_{max} (nm, ϵ (M⁻¹ cm⁻¹)): 454(5290), 559(sh). Anal. for Ru₂C₄₈N₈O₄H₅₀I₂, found(calcd): C, 44.47(44.54); H, 4.00(3.89); N, 8.46(8.66). Cyclic voltammogram [$E_{1/2}$ /V, ΔE_p /V, $i_{\text{backward}}/i_{\text{forward}}$]: B, 0.410, 0.072, 0.89; E_{pc} (C), -0.790 V; E_{pa} (E), -0.446 V.

Preparation of cis-Ru₂(DmAniF)₂(DMBA-4-C₂Fc)₂Cl (8). Compound 8 was synthesized from treating 7 with 8 equiv of ferrocenylacetylene using a procedure identical to that for 3b. Yield: 52%. Data for 8: R_f (ethyl acetate/hexane/triethylamine = 3/6/1), 0.51. MS-FAB (m/e , based on ¹⁰¹Ru): 1425 [M⁺ - Cl]. Vis-NIR, λ_{max} (nm, ϵ (M⁻¹ cm⁻¹)): 453(7990), 650(sh). Anal. for Ru₂C₇₂N₈O₄H₆₈Fe₂Cl, found(calcd): C, 59.02-(59.29); H, 5.05(4.70); N, 7.67(7.68). χ_{mol} (corrected) = 5.98 × 10⁻³ emu, μ_{eff} = 3.78 μ_B . Cyclic voltammogram [$E_{1/2}$ /V, ΔE_p /V, $i_{\text{backward}}/i_{\text{forward}}$]: B, 0.389, 0.061, 0.49; F, 0.693, 0.066, 0.88; E_{pc} (C), -0.845 V; E_{pc} (D), -1.749 V.

Preparation of cis-Ru₂(DmAniF)₂(DMBA-4-C₂Fc)₂(C₂-Ph)₂ (9). This was synthesized using the same procedure as that for 5 with the starting material 2 replaced by 8. Data for 9: yield 46%. R_f (ethyl acetate/hexanes = 1/5), 0.38. MS-FAB (m/e , based on ¹⁰¹Ru): 1628 [M⁺]. ¹H NMR: 8.22 (s, 2H, NCHN), 7.56–7.59 (d, 4H, aromatic), 7.05–7.11 (m, 8H, aromatic), 6.94–6.96 (m, 8H, aromatic), 6.69–6.70 (t, 2H, aromatic), 6.63–6.69 (m, 8H, aromatic), 6.52–6.55 (d, 4H, aromatic), 4.52–4.53 (t, 4H, ferrocenyl), 4.23–4.27 (m, 14, ferrocenyl), 3.36 (s, 12H, NCH₃), 3.62 (s, 12H, OCH₃). Cyclic voltammogram: Vis-NIR, λ_{max} (nm, ϵ (M⁻¹ cm⁻¹)): 517-(15 670), 908(1110). Anal. for C₈₈H₇₈Fe₂N₈O₄Ru₂·C₆H₁₄, found(calcd.): C, 65.75(65.96); H, 5.22(5.42); N, 6.40(6.55). Cyclic voltammogram [$E_{1/2}$ /V, ΔE_p /V, $i_{\text{backward}}/i_{\text{forward}}$]: E_{pa} (A), 1.110 V; B, -0.673, 0.065, 0.89; E_{pc} (C), -1.741; F, 0.756, 0.073, 0.70.

Preparation of cis-Ru₂(DmAniF)₂(DMBA-I)₂(C₂Ph)₂ (10). Compound 10 was prepared using the same procedure as that for 5 with compound 7 (0.25 g, 0.19 mmol) instead of 2. Compound 10 was isolated as a dark red microcrystalline material (0.15 g, 51%). Data for 10: R_f (ethyl acetate/hexanes = 1/5), 0.45. MS-FAB (m/e , based on ¹⁰¹Ru): 1463 [M⁺]. Vis-NIR, λ_{max} (nm, ϵ (M⁻¹ cm⁻¹)): 521(14 720), 920(1440). Anal. for C₆₄H₆₀N₈O₄I₂Ru₂·0.5C₆H₁₄, found(calcd): C, 54.18(54.46); H, 4.44(4.55); N, 7.09(7.44). ¹H NMR: 8.20 (s, 2H, NCHN), 7.80–7.81 (d, 4H, aromatic), 7.04–7.12 (m, 8H, aromatic), 6.94–6.95 (t, 4H, aromatic), 6.73 (s, 2H, aromatic), 6.62–6.65 (d, 12H, aromatic), 6.49–6.51 (d, 4H, aromatic), 3.31 (s, 12H, NCH₃), 3.52 (s, 12H, OCH₃). Cyclic voltammogram [$E_{1/2}$ /V, ΔE_p /V, $i_{\text{backward}}/i_{\text{forward}}$]: E_{pa} (A), 0.805 V; B, -0.646, 0.065, 0.89; E_{pc} (C), -1.762.

X-ray Data Collection, Processing, and Structure Analysis and Refinement. Single crystals were grown via slow evaporation of either an ethyl acetate/hexanes solution (1 and 10), a hexanes solution (4a and 5), a CH₂Cl₂ solution (6), or a toluene/hexanes solution (9). The X-ray intensity data were measured at 300 K on a Bruker SMART1000 CCD-based X-ray diffractometer system using Mo K α (λ = 0.71073 Å). Thin plates of dimension 0.40 × 0.20 × 0.20 mm³ (1), 0.30 × 0.24 × 0.07 mm³ (4a), 0.27 × 0.05 × 0.03 mm³ (5), 0.50 × 0.13 × 0.06 mm³ (6), 0.60 × 0.17 × 0.10 mm³ (9), and 0.48 × 0.36 × 0.20 mm³ (10) were used for X-ray crystallographic analysis. Crystals were cemented onto a quartz fiber with epoxy glue. Data were measured using omega scans of 0.3° per frame such that a hemisphere (1271 frames) was collected. No decay was indicated for any of six data sets in the re-collection of the first 50 frames at the end of each data collection. The frames were integrated with the Bruker SAINT software package using a narrow-frame integration algorithm, which also corrects for the Lorentz and polarization effects.³⁹ Absorption corrections were applied using SADABS supplied by George Sheldrick.

The structures were solved and refined using the Bruker SHELXTL (Version 5.03) software package⁴⁰ in the space

groups $P\bar{1}$ for crystals **1**, **4a**, **6**, and **10**, $P2_1/n$ for **5**, and $P2_1/c$ for **9**. Positions of all non-hydrogen atoms of diruthenium moieties were revealed by the direct method. In the cases of crystals **1**, **4a**, and **5**, the asymmetric unit contains one independent molecule; in the case of crystal **6**, the asymmetric unit contains one independent molecule with one H₂O molecule coordinating to its axial position and one CH₂Cl₂ solvate molecule; in the case of crystal **9**, the asymmetric unit contains one independent molecule and one THF solvate molecule; in the case of crystal **10**, the asymmetric unit contains two independent molecules. With all non-hydrogen atoms being

(39) SAINT V 6.035 Software for the CCD Detector System; Bruker-AXS Inc., 1999.

(40) (a) SHELXTL 5.03 (WINDOW-NT Version), Program Library for Structure Solution and Molecular Graphics; Bruker-AXS Inc., 1998. (b) Sheldrick, G. M. SHELXS-90, Program for the Solution of Crystal Structures; University of Göttingen: Germany, 1990. (c) Sheldrick, G. M. SHELXL-93, Program for the Refinement of Crystal Structures; University of Göttingen: Germany, 1993.

anisotropic and all hydrogen atoms in calculated position and riding mode the structure was refined to convergence by the least-squares method on F^2 , SHELXL-93, incorporated in SHELXTL.PC V 5.03.

Acknowledgment. We are grateful to the National Science Foundation (CHE0242623) and Office of Naval Research (N00014-03-1-0531) for providing financial support.

Supporting Information Available: Text giving details of the attempted synthesis of **4a** from **5**, vis-NIR spectra of compounds **1–10**, and electrochemistry of compounds **3b**, **4b**, **8**, and **9**, and X-ray crystallographic files in CIF format for compounds **1**, **4a**, **5**, **6**, **9**, and **10**. This material is available free of charge via the Internet at <http://pubs.acs.org>.

OM050068T